AD-A058 812 SOUTH DAKOTA SCHOOL OF MINES AND TECHNOLOGY RAPID CI--ETC F/G 7/4
SAPPHIRE ATOMIC HYDROGEN DISSOCIATOR BULB DESIGN.(U)
MAY 78 C L GRUBER N00173-77-C-0134

UNCLASSIFIED NL

| OF |
AD
A058 812

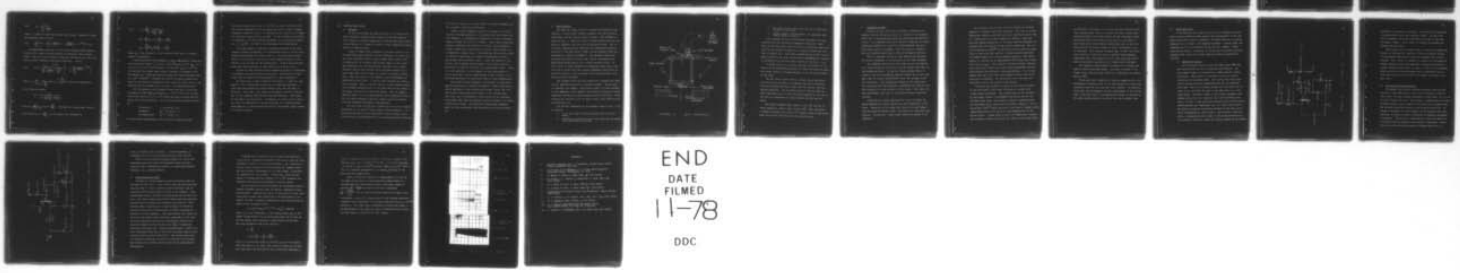

END
DATE
FILMED
11-78
DDC

(12) B.S.

LEVEL II

537652 (6)

(6) SAPPHIRE ATOMIC HYDROGEN DISSOCIATOR BULB DESIGN

(9) FINAL REPORT,

CONTRACT N00173-77-C-0134 (15)

Prepared for

NAVAL RESEARCH LABORATORY

WASHINGTON, D.C.

(10) submitted by

Dr. Carl L. Gruber

Electrical Engineering Department

SOUTH DAKOTA SCHOOL OF MINES AND TECHNOLOGY

RAPID CITY, SOUTH DAKOTA

New 410 848

(11) May 78

(14) 32 p.

ABSTRACT

Design criteria and fabrication details of a 2-inch diameter by 2 inch high circular cylinder hydrogen RF discharge dissociator bulb are developed and described. A rate equation model is developed to determine operating parameter relationship to be investigated during the testing program phase to follow. Results from testing of a similar pyrex dissociator bulb are presented.

TABLE OF CONTENTS

I. Introduction

Conventional wisdom dictates that the most efficient and long-lived discharge dissociator bulb material is pyrex glass. Although many factors contribute to the dissociation efficiency of hydrogen atom source, the primary controlling factor internal to the system is the wall (surface) recombination coefficient, . Pyrex under certain conditions seems to possess a very low value of atomic hydrogen surface recombination coefficient (usually following a suitable conditioning period lasting 48 hours or more). Moreover, lifetimes of pyrex bulbs have been obtained in excess of five years.[1] We can define bulb lifetime as the period of time over which the output atomic flux drops to 1/2 its initial value under constant environmental conditions.

The surface recombination coefficient is here defined as the fraction of atoms striking the wall surface, due to random thermal motion in the gas volume, that recombine to form molecular hydrogen at the container walls. Specification of the recombination process is complicated by first the possibility of long residence time of atomic hydrogen at or near the surface prior to actual recombination and, secondly, surface adhesion of recombined molecules prior to remission into the gas volume. Factors contributing to the above processes include physical adsorption, chemisorption, permeation, and high surface mobility of both the atomic and molecular species. These factors are further complicated by the presence of unknown surface contamination, various impurities in the glass (perhaps minor constituents of the glass material is a more appropriate term), and

a high UV radiation flux from the discharge itself. The latter factor may indeed prove to be the most significant because UV radiation has a very large absorption coefficient in pyrex, causing heating at the surface, and also is energetically capable of photo dissociating and/or exciting molecular hydrogen attached to the surface.

It is known that minor surface contamination from organic substances, apparently resulting in high surface concentrations of carbon,[2] contribute to a greatly increased recombination coefficient. The most likely cause of this problem is the high affinity of a pyrex glass surface for organic solvents and water vapor. If the glass is baked prior to use as a discharge bulb, it is likely the absorbed solvents are cracked to form free carbon, while if an unbaked bulb is used, the active discharge probably degasses the absorbed organics from the wall without totally decomposing the molecular structure. A similar situation concerns the use of natural gas (rather than hydrogen) when working the glass stock to form the usual discharge bulb geometry, organic residue could remain in the material.[3] At best, only qualitative experimental verification of the preceding conjectures exist.

Cumulative degradory effects on surface recombination coefficient over a period of time measured in years are consistently observed. Qualitative chemical analysis of bulb wall materials after long exposure to the active hydrogen discharge indicate structural changes in the surface material including reduction of alkaline oxides and formation in some cases of complex hydrides. All of these

wall heating due to surface absorption (attenuation coefficient in pyrex, $\beta > 10^4/cm$) of the radiation. Secondly, the impurity concentration of a single crystal Al_2O_3 surface as is to be used here is very low. This should remove or reduce to a minimum the effects of long term chemical alteration of the surface leading to increased surface recombination rates. In addition, crystalline Al_2O_3 has a very tightly bound crystal structure which should result in a high activation energy for adsorption of hydrogen. Finally, a well polished sapphire surface should exhibit a ratio of actual geometric surface area near unity (pyrex glass has 1.2)[7] leading to minimum available recombination area. This latter factor does not favor use of polycrystalline alumina ceramic for which the ratio approaches 100.

II. Theory

Although it may be neither entirely correct nor complete, it is useful to set forth a phenomenological theory describing the surface and volume reactions involving atomic hydrogen. The theory takes the form of a set of rate equations. This set of equations should include as many known reaction phenomena as could be expected to apply. Unfortunately, rate constants for atomic hydrogen surface adsorption and recombination are not known for most materials so we must speculate that the former is not more than an order of magnitude different from that for molecular hydrogen, and the latter is the same order of magnitude as that for pyrex. Molecular hydrogen

parameters themselves are only sparsely reported in the literature, data being primarily for metal surfaces. We begin by defining a few terms.

Let $N_w - \frac{\text{atoms}}{cm^2}$ be the surface density of adsorbed hydrogen atoms with N_o the limiting or saturation value. For atoms, the density constituting a single monolayer should be approximately $N_o \approx 10^{15}$ atoms/cm^2, while for molecular hydrogen we have $N_o \approx 7(10^{14})$ molecules/cm^2. Assuming multilayer formation and chemisorption are possible on some materials, N_o may be considerably larger than the monolayer value. In any case, we define the fractional surface coverage of the wall as $\theta = \frac{N_w}{N_o}$.

The number of atoms striking unit area of wall surface from the gas phase is $\frac{n_H \bar{v}}{4}$ atoms/sec·cm^2, where n_H is the volume density of atoms and $\bar{v}$ their mean speed. Normalizing this to the saturation surface density we define $Y = \frac{n_H \bar{v}}{4N_o}$.

A bulb of volume V is assumed with net inside wall surface area A_w. The total effective area of gas exit and entrance ports (effusers) is A_o. The wall surface sticking coefficient is unity over the port areas and is taken as S times the fraction of wall area not saturated by adsorbed gas, $(1-\theta)$. Lifetime of an adatom is taken to be τ_s, a function of the surface bonding energy, E_a, such that $\tau_s \cong (10^{-13})\exp(+\frac{E_a}{kT_s})$sec, where T_s is the wall surface temperature. We will assume initially (subject to reservations) first order recombination of atomic hydrogen on the walls with a probability γ per wall collision. Previous research has indicated

phenomena are accompanied by a visible darkening of the glass. Surface contamination accelerates the above processes as previously noted.

Various surface coatings can be added to surfaces to affect a reduction in surface recombination coefficient, notably teflon, Drifilm, and metaphorphoric acid, all of which are eventually decomposed by the active discharge products.

Mandl and Shalop[3] have measured a first order (assumed) surface recombination coefficient for Corning 7070 glass which is very similar to Pyrex 7740 and found a value $\gamma = 5.\text{-}10.(10^{-5})$.

Although others[4,5,6] have measured values close to this, there is a serious question whether any of these experiments allowed sufficient time for the surface to equilibrate with the discharge consituents. Moreover, experimental conditions have varied widely. In summary, the process of atomic recombination of hydrogen on surfaces is very poorly understood.

"Pure" silicon vessels composed of vycor or fused quartz are even less well understood, but it is apparent from a number of references that the recombination coefficients on these materials is about one order of magnitude higher than that for pyrex,[3] all other things perhaps not equal. This leads to a considerably lower dissociation efficiency.

As will be shown in the next section, the potential advantages of a sapphire discharge vessel lie first in the fact that the material is relatively transparent to the short wavelength UV radiation emanating from the discharge. This has the effect of reducing

this to be the case,[8] although wall surface contamination is surely a contributing factor in most cases reported. Finally we assume volume recombination is negligible[9] in the pressure range of interest here, and dissociation of molecular hydrogen is a purely volume process occurring at a rate of $\beta V N_{H_2}$ atoms/sec where β depends upon the RF discharge electron temperature and density.

Utilizing the above physical processes we can write rate equations for Y and θ as,

(a) $$\left(\frac{4V}{\bar{v}A_w}\right)\frac{dY}{dt} = -Y\left(s + \frac{A_o}{A_w} - (s-\gamma)\theta\right) + \frac{\theta}{\tau_s} + \frac{\beta V}{N_o A_w} N_{H_2}$$

(2) $$\frac{d\theta}{dt} = -\theta\left[(s+\gamma)Y + \frac{1}{\tau_s}\right] + sY$$

Solving for (1) and (2) for the final steady state conditions for which $\frac{dY}{dt} = \frac{d\theta}{dt} = 0$, we get,

$$-2\gamma\theta_{ss}Y_{ss} - \frac{A_o}{A_w}Y_{ss} + \frac{\beta V}{N_o A_w} N_{H_2} = 0$$

or $$Y_{ss} = \frac{\frac{\beta V}{A_w}\frac{N_{H_2}}{N_o}}{A_o/A_w + 2\gamma\theta_{ss}}$$

with the steady-state dissociation level given as

(3) $$\left(\frac{n_H}{N_{H_2}}\right)_{ss} = \frac{4\frac{\beta V}{\bar{v}A_w}}{A_o/A_w + 2\gamma\theta_{ss}}$$

Clearly the determining factors in achieving high dissociation percentages are γ and θ_{ss}, both of which are sensitive to the type of material on the discharge bulb walls. This, of course, assumes A_o/A_w is not the limiting factor. Anything serving to reduce these quantities will provide a more efficient dissociator. Now,

$$(4) \qquad \theta_{ss} = \frac{SY_{ss}}{(s+\gamma)Y_{ss} + 1/\tau_s}$$

so that very small τ_s minimizes θ_{ss}. This is the case with a teflon surface where $\tau_s \rightarrow 0$. On the other hand, large dissociation rates (βN_{H_2}) allow $\theta_{ss} \rightarrow \frac{s}{s+\gamma}$, near unity (assuming values for $s \approx 1/2$ and $\gamma \approx 5\times10^{-5}$ as reported in the literature for pyrex glass) with the result that

$$(5) \qquad \frac{n_H}{N_{H_2}} \approx \frac{\frac{4\beta V}{\bar{v}A_w}}{A_o/A_w + 2\frac{\gamma s}{s+\gamma}} \approx \frac{\frac{4\beta V}{\bar{v}A_w}}{A_o/A_w + 2\gamma}$$

If $A_o/A_w \ll 2\gamma$ as is the case for the usual discharge bulb, the system is wall recombination dominated.

In the above system of equations most of the constants (s, γ, τ_s, N_o, and β) are either completely unknown or known to within an

order of magnitude for but a few materials. β, of course, is relatively independent of the wall material. Within reasonable limits of accuracy $s \approx 1$, and N_o can be written in terms of integral number of monolayers of adatoms. τ_s can be found if the binding energy can be determined by varying bulb wall temperature. This factor probably determines the dissociation efficiency over the long term. In general for metals τ_s is very long resulting in large surface coverage and rapid recombination, while on inactive surfaces which could include sapphire, τ_s is very small, perhaps on the order of 10^{-4}-10^{-8} sec, leading to a low surface recombination rate. The latter effect could appear in some cases after an initially formed chemisorbed layer "passivates" the surface.

In any case, the difficulty surrounding lack of determination of the constants can be resolved if transients following striking or extinction of the active discharge in the dissociator bulb can be observed. Assuming "passivation" of the surface occurs very rapidly and the layer is strongly bound, additional adsorption follows Eqs. (1,2).

Initially we will assume in solving (1,2) that desorption is negligible, $\tau_s \gg 1$. It follows that the solution for (2) is

$$\theta(t) = \frac{s}{s+\gamma}\left(1 - e^{-(s+\gamma)\int_o^t Y(\tau)d\tau}\right) \tag{5}$$

Substituting this into (1) we have

$$\frac{4V}{\bar{v}A_w}\frac{dY(t)}{dt} = -Y(t)\left[\left(\frac{A_o}{A_w} + \frac{2s\gamma}{s+\gamma}\right) + s\left(\frac{s-\gamma}{s+\gamma}\right)e^{-(s+\gamma)\int_o^t Y(\tau)d\tau}\right] + \frac{\beta V}{N_o A_w} N_H \tag{6}$$

Defining $(s+\gamma)\int_o^t Y(\tau)d\tau = F(t)$ and $\frac{\beta V}{N_o A_w} N_{H_2} = X(t)$, a given source function (actually taken as step function excitation), we can evaluate the transient response of the system from

$$(7) \qquad \frac{4V}{\bar{v}A_w}\ddot{F}(t) = -\dot{F}(t)\left[\left(\frac{A_o}{A_w} + \frac{2s\gamma}{s+\gamma}\right) + s\left(\frac{s-\gamma}{s+\gamma}\right)e^{-F(t)}\right] + X(t)$$

During the initial transient period $F(t) \ll 1$, so

$$(8) \qquad \frac{4V}{\bar{v}A_w}\ddot{F}(t) = -\dot{F}(t)\left(s + \frac{A_o}{A_w}\right) + X_o$$

The solution of (8) with $\dot{F}(t) \alpha U(t) \alpha n_H(t)$ has a transient time constant, τ_i, given by

$$(9) \qquad \tau_i = \frac{4V}{\bar{v}A_w\left(s + \frac{A_o}{A_w}\right)} \text{ sec}$$

and a pseudo steady-state value of $Y(t)$ with $t_o \gg \tau_i$ of

$$(10) \qquad Y_i(t_o) \cong \frac{X_o}{\left(s + \frac{A_o}{A_w}\right)(s+\gamma)}$$

From (10) we get the intermediate value for n_H as

$$(11) \qquad n_H(t_o) \approx \frac{4\beta V}{s^2 \bar{v} A_w} N_{H_2}$$

assuming $s \gg \frac{A_o}{A_w}, \gamma$.

Now if $N_{H_2} \leq N_o$, this pseudo steady state value is given by $Y_i(t) \lesssim 1$. The exponential term remains near unity and a period ensues during which $Y(t)$ very slowly increases toward the final true steady state value,

$$(12) \qquad Y_{ss} = \frac{X_o}{\frac{A_o}{A_w} + \frac{2s\gamma}{s+\gamma}}$$

some five orders of magnitude larger than $Y_i(t_o)$! Equation (7) may be integrated once to yield

$$(13) \qquad \frac{4V}{\bar{v}A_w}\dot{F}(t) + \left(\frac{A_o}{A_w} + \frac{2s\gamma}{s+\gamma}\right)F(t) + s\frac{(s-\gamma)}{(s+\gamma)}\left(1 - e^{-F(t)}\right) = X_o t$$

An approximate solution to (13) can be obtained which qualitatively gives results observed during the "burn-in" time of pyrex bulbs. This is a short duration transient followed by the long slow rise in atomic hydrogen production efficiency. We get

$$(14) \qquad Y(t) = \frac{X_o(1 - e^{-t/\tau_1})}{\left(\frac{A_o}{A_w} + \frac{2s\gamma}{s+\gamma}\right)\left(s + \frac{A_o}{A_w}\right)^2}\left[s - \frac{s}{s + \frac{A_o}{A_w}}\frac{(s-\gamma)}{(s+\gamma)}e^{-t/\tau_2}\right]$$

where $\tau_1 = \frac{4V}{\bar{v}A_w}\frac{1}{\left(s + \frac{A_o}{A_w}\right)}$ and $\tau_2 = \frac{s + \frac{A_o}{A_w}}{X_o}$ sec with the steady-state value being as before,

$$Y_{ss} = \frac{X_o}{\left(s + \frac{A_o}{A_w}\right)\left(\frac{A_o}{A_w} + \frac{2s\gamma}{s+\gamma}\right)}$$

with $X_o = \frac{\beta V}{N_o A_w} N_{H_2}$ and $Y = \frac{n_H \bar{v}}{4N_o}$. Defining the steady-state dissociation fraction, $\alpha = \frac{n_H}{N_{H_2}}$, we can evalute the constants as

$$(15) \qquad \tau_2 = \frac{4N_o}{\alpha N_{H_2}} \frac{1}{\bar{v}\left(\frac{A_o}{A_w} + \frac{2s\gamma}{s+\gamma}\right)}$$

$$\beta V = \frac{\alpha \bar{v}}{4}(sA_w + A_o)\left(\frac{A_o}{A_w} + 2\,\frac{s\gamma}{s+\gamma}\right)$$

$$K_m = \frac{\alpha N_{H_2}}{N_m} \gamma_{ss} \left(\frac{\bar{v}}{4}\right)\left(\frac{A_o}{A_w} + 2\,\frac{s\gamma}{s+\gamma}\right)$$

where K_m is the thickness of the adsorbed atom layer in integral number of monolayers.

Inserting values corresponding to usual experimental conditions for pyrex 7740, namely $s \cong 1$; $\gamma \cong 5 \{10^{-5}\}$; $A_o/A_w \cong 10^{-4}$; $p_{H_2} \cong 0.1$ torr; $\alpha \cong 0.1$; $\bar{v} \cong 6(10^{-4})$ cm/sec; $V \cong 100$ cm^3; $T_2 \cong 5 \times 10^4$ sec; we find that the steady state surface coverage corresponds to approximately $K_m = 26000$ monolayers assuming one atomic monolayer has $N_o \cong 10^{15}$ atoms/cm^2. Although this result is almost ridiculously large we can provide confirmation since using this value for N_o, the dissociation rate becomes $\beta V = 15$ or $\beta = .15$ atoms/molecule/sec.

For the plasma we can estimate β since the rate is given approximately by $\beta \cong 2\sigma_i \bar{v}_e n_e$ where $\sigma_i = 5 \times 10^{-17}$ cm^2 is the ionization cross section, $\bar{v}_e \cong 5 \times 10^6$ cm/sec the mean electron velocity, and n_e the electron density. If the dissociation reactions proceed as

(ionization)	$e + H_2 \rightarrow H_2^+ + 2e$
(exchange)	$H_2^+ + H_2 \rightarrow H_3^+ + H$
(recombination)	$H_3^+ + e \rightarrow H_2 + H$

we would expect approximately two atoms per ionization event.

Inserting values we get $n_e \cong 3 \times 10^8/cm^3$, a value consistent with the RF power absorbed by the discharge and the fact that a plasma resonance condition ($\omega_p \cong \omega$) is observed in the vicinity of 110 MHz. For the above n_e we get $f_p = 150$ MHz. If the resonance corresponds to coupling to the first Dattner Resonance of a cylindrical plasma, f_o, $f_o = f_p/\sqrt{2} = 106$ MHz in good agreement with measurements.

The large amount of hydrogen ultimately adsorbed on the bulb surface actually corresponds to a significant fraction of the total hydrogen flow during the burn-in time τ_2. The resulting pressure drop ($\sim 15^o/o$) after initiation of the discharge becomes a good measure of N_o attained in the steady-state. In fact large pressure drops have been observed, in some cases up to a factor of 2.

Finally we have derived several parameters useful in evaluating a potential dissociator bulb wall material. Observation of transient effects should allow determination of these parameters.

We would like to have a material with small τ_s, small N_o, and small γ, all of which can be directly or indirectly measured. A bulb with these properties should exhibit long life and high efficiency. If N_o and τ_s are large we can expect a shorter lifetime due to slow chemical reaction with the wall material. With large we can expect low efficiency. In sapphire we would a priori expect the first two conditions to be met resulting in a reduced surface concentration, θ, and reducing the effects of possibly larger values of γ than for pyrex.

III. SAPPHIRE BULB DESIGN

A. Material

As far as possible the shape and size of the dissociator bulb using pure aluminum oxide (Al_2O_3) as the wall material will conform to typical dimensions of conventional pyrex bulbs. In this manner it is hoped to obtain a valid comparison between pyrex and sapphire bulbs.

Al_2O_3 is commercially available in several forms for all of which high purity material can be obtained if so specified. The least expensive form is Al_2O_3 ceramic which lends itself to fabrication of virtually any desired shape or size vessel. Unfortunately, the microcrystalline structure of a ceramic material such as this results in an irregular surface with a very large value for the ratio of actual to geometric surface area. Thus the effect of any surface reaction phenomena are amplified by this ratio. To resolve this problem the surface can be glazed. This, of course, results in the surface properties becoming characteristic of the glaze and not the underlying Al_2O_3, even for very thin film glazes. Only if sapphire material proves to be an exceptionally non-recombinative material for atomic hydrogen could the ceramic form be acceptable as an RF discharge dissociator bulb material.

The best form of Al_2O_3 for a definitive test of its surface properties is, of course, clear single crystal sapphire. Very high material purity can be maintained using the usual Czochralski crystal growth method with very uniform crystal structure

in boules as large as or larger than 8" D being obtainable under carefully controlled conditions.

Single crystal sapphire, grown in the shape of a hollow cylinder with approximately 2.5 mm thick walls and 1-inch outside diameter, is obtainable at moderate cost with continuous segment lengths in excess of 6 inches. From a purely material property standpoint this material is ideal, since naturally formed crystal faces constitute the entire inner surface of a cylindrically shaped vessel. Unfortunately, grown boules tend to exhibit a high degree of surface irregularity on both a macroscopic and microscopic scale. Since the surface is not smooth, some gringind and polishing of the surface would be necessary to render it suitable as a dossicoator vessel. Since it is not possible to work sapphire as one would quartz or silica materials, even at temperatures in the vicinity of its bulk melting point, all fabrication must be done mechanically.

Pure single crystal sapphire is available in solid homogeneous boules up to 8 inches in diameter. These large boules can be machined to form virtually any shape vessel, and with any desired orientation with respect to the crystal axes. Since the costs of machining a solid boule are not substantially higher than that for growing a hollow cylinder, the former solution was chosen. The boule was produced and component parts for the cylindrical bulb fabricated by Crystal Systems, Inc.

B. Bulb Geometry

The bulb was formed from five separately fabricated components, a hollow right circular cylinder, two flat circular end plates, an inlet and an outlet effuser. The assembly is shown in Fig. 1. Only the outlet (H beam) effuser was not composed of sapphire, but this will be discussed later. All of the other components were obtained from immediately adjacent sections of one high purity single crystal sapphire boule approximately 4 inches in diameter. This perhaps unnecessary procedure was taken to assure that crystal orientation was maintained between pieces to be sealed together later. In fact, prior to final assembly the components parts were x-ray oriented to assure that the various components were placed in position similar to that occupied in the original boule from which they were obtained.

The original boule also was checked for twinning and other crystal imperfections prior to machine working. The presence of twinning, for example, could cause trouble in final assembly of the components since sapphire has slightly different thermal expansion coefficients along different axial directions. Final assembly was carried out by the Maser Group at RCA Laboratories in Princeton, N.J.

The various components in the assembly shown in Fig. 1 are as follows:

1. 2 x 2 inch right circular cylinder with 0.10 inch walls,
2. end plates 2 inch OD x 0.040 inch thick (in the future 0.10 inch would be chosen),

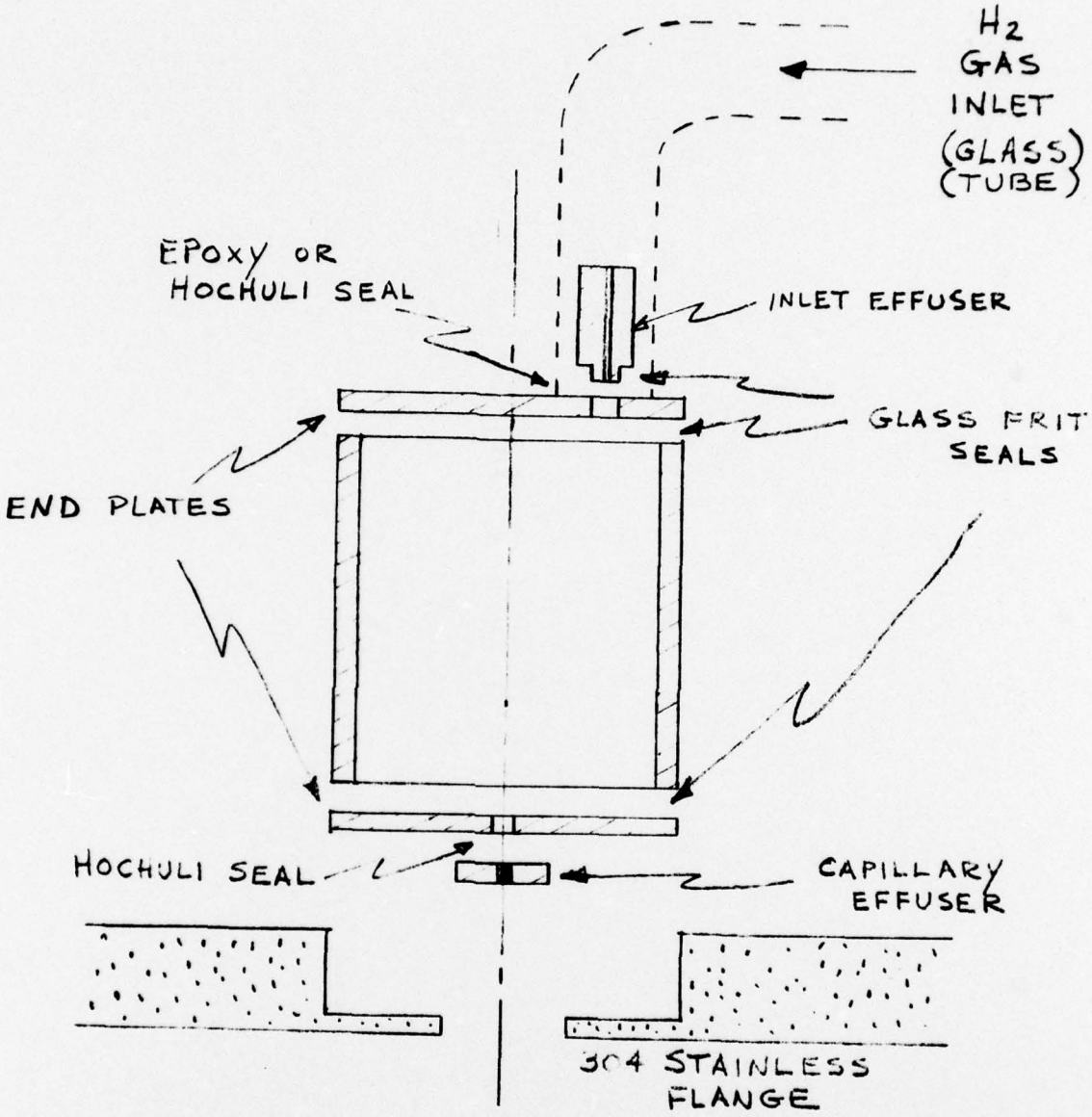

FIGURE 1 BULB ASSEMBLY

3. gas inlet effuser tube, 0.25 inch OD x 0.040 inch ID and 0.5 inch long,

4. H beam effuser, 50 μm diameter, 91 capillary tube effuser array in pyrex.

The cylindrical piece was partially polished to a non-scratech free but optically transparent condition. Both faces of the end plates were polished to an optical grade finish, but no attempt was made for a totally scratch free surface in either case. With these precautions an actual to geometric surface area ratio for H surface recombination purposes is estimated to be no more than a factor of two ($A_w' = 2\ A_w$).

As shown in Fig. 1, a 0.125 inch hole is drilled in the center of the downstream end plate to allow the attached capillary array effuser a minimum exposure to the active discharge in the bulb.

The gas inlet effuser tube is located in an off-center position in the top plate to eliminate any direct molecular flow path through the bulb volume from the inlet to the exit effuser apertures. The end plate hole for the gas inlet effuser tube mates with a 0.040 inch deep shoulder at the end of the tube to strengthen the joint between the tube and the plate.

The final assembled bulb volume is 83.4 cm^3 with an internal geometric surface area of 105.8 cm^2. This represents a volume-to-surface area ratio 17% smaller than an equivalent bulb with curved ends fabricated from pyrex glass.

C. Component Assembly

Despite the care with which individual components are handled, serious mechanical stress is induced in all sapphire pieces due to machining and polishing operations during fabrication. All component parts were therefore annealed in a high temperature furnace for a period of approximately one and a half months prior to assembly. This was done as a result of previous problems experienced at RCA with sapphire material.

Prior to assembly the pieces were again x-ray oriented for precise alignment of optical axes in the final assembly.

The component pieces were all joined in one low temperature fusing operation using iron free low alkali glass frit as the bonding material. As the frit flowed during fusion it tended to wet the surrounding sapphire surface up to 1/16 inch away from the joints, particularly where the cylinder joins the end plates. This unexpected flowing of the fused glass frit could provide some problems in modifying the material surface properties in the vicinity of the joints. The effects on bulb performance will have to be assessed during evaluation testing.

Following the fusing operation the entire assembly was again annealed by slowly reducing the oven temperature to ambient. Integrity of all joints was tested by visual inspection and using polarized light. All seem to be continuous and uniform. Testing under high vacuum conditions remains to be completed.

Two alternate and possibly superior methods for forming sapphire to sapphire seals were explored. The first is a high temperature expansion matched glass frit seal which can be done on a custom basis in a high temperature furnace. Questionable and unknown properties of the glass involved (produced in Germany) make the success of this process uncertain. The second, developed by NASA[10] for Rb maser cavities uses an Al_2O_3/TiO_2 frit material that provides virtually perfect matching of thermal properties to bulk sapphire material. The fusion process is carried out at approximately 25°C below the softening point of Al_2O_3. This requires extremely careful temperature control but results in a seal indistinguishable from the bulk material and extremely strong and uniform. It is recommended that any future work with sapphire utilize the latter fabrication technique. The facilities to do this were not available to us at the outset of the project.

The pyrex exit effuser is sealed to the lower end plate of the bulb using a thin layer of epoxy as is usual with similar pyrex assemblies. The central hole in the end plate is just large enough to accommodate the entire area of the capillary tube array. Here again a superior bonding method was discovered after fabrication was nearly complete. This is the Hochuli seal[11] which utilizes a thin film of indium solder sandwiched between thin layers of gold predeposited on the mating pieces. Indium flows at very low temperature eliminating thermally induced stress and pro iding a very strong bond.

No measurable outgassing is observed from this entirely metal seal, whereas epoxy layers, no matter how thin, yields some volatile products over long periods of time following curing. The Hochuli seal leaves only a very thin (< 2 μm) layer of metal exposed to the discharge volume which can, in fact, be recessed from the active volume at least a millimeter or so if necessary. This sealing technique may, in fact, be effectively utilized in pyrex as well as sapphire bulb assembly, especially since some suspicion exists that epoxy may ultimately be partially responsible for limited bulb lifetimes.

The completed bulb assembly is mounted in a suitably machined 4-inch Varian UHV flange. The bulb is bonded to the flange using torr-seal epoxy cured at a temperature of approximately 140^{o}F.

The Hz gas inlet connection is made as shown in Fig. 1 by epoxying an 8 mm pyrex tube to the top end plate in a position concentric with the 0.25 inch gas inlet effuser. It should be noted that this arrangement allows a measurement of the H atom flux at the inlet part if an appropriate sensor is inserted in the glass tubing opposite the end of the inlet effuser tube.

IV. Pyrex Bulb Tests

A conventional pyrex bulb dissociator test program was initiated to provide baseline data against which performance of the sapphire dissociator could be compared. The pyrex bulb was of similar dimension (2 x 2 inch) to the sapphire assembly. Several other new components were to be evaluated during the test, namely, a VMOS power FET RF source, oscillator, an electrolytic molecular hydrogen generator and a thin foil atomic hydrogen surface recombination detector.

A. VMOS RF Oscillator

Two oscillator circuits using the VMP-1 power VMOS FET have been evolved for use in dissociator RF sources. The first shown in Fig. 2 is basically a common emitter Colpits oscillator. This circuit is currently in use as a source oscillator for the pyrex bulb. This circuit has been extensively tested using both simulated loads and the discharge bulb load. With a 24 V supply voltage the oscillator can deliver up to 5 W output RF power at 100 MHz with 6 to 8 W dc input power. The power output is only weakly dependent upon loading across the coil terminals for load resistance from 1000 Ω to 50 KΩ. Load power was measured using a substitution method whereby the temperature rise in a given load resistor was used to establish equivalence between the RF power level and a calibratable dc power source. This circuit, unfortunately, is unbalanced with respect to RF ground potential and is seriously limited in output RF voltage, making the discharge

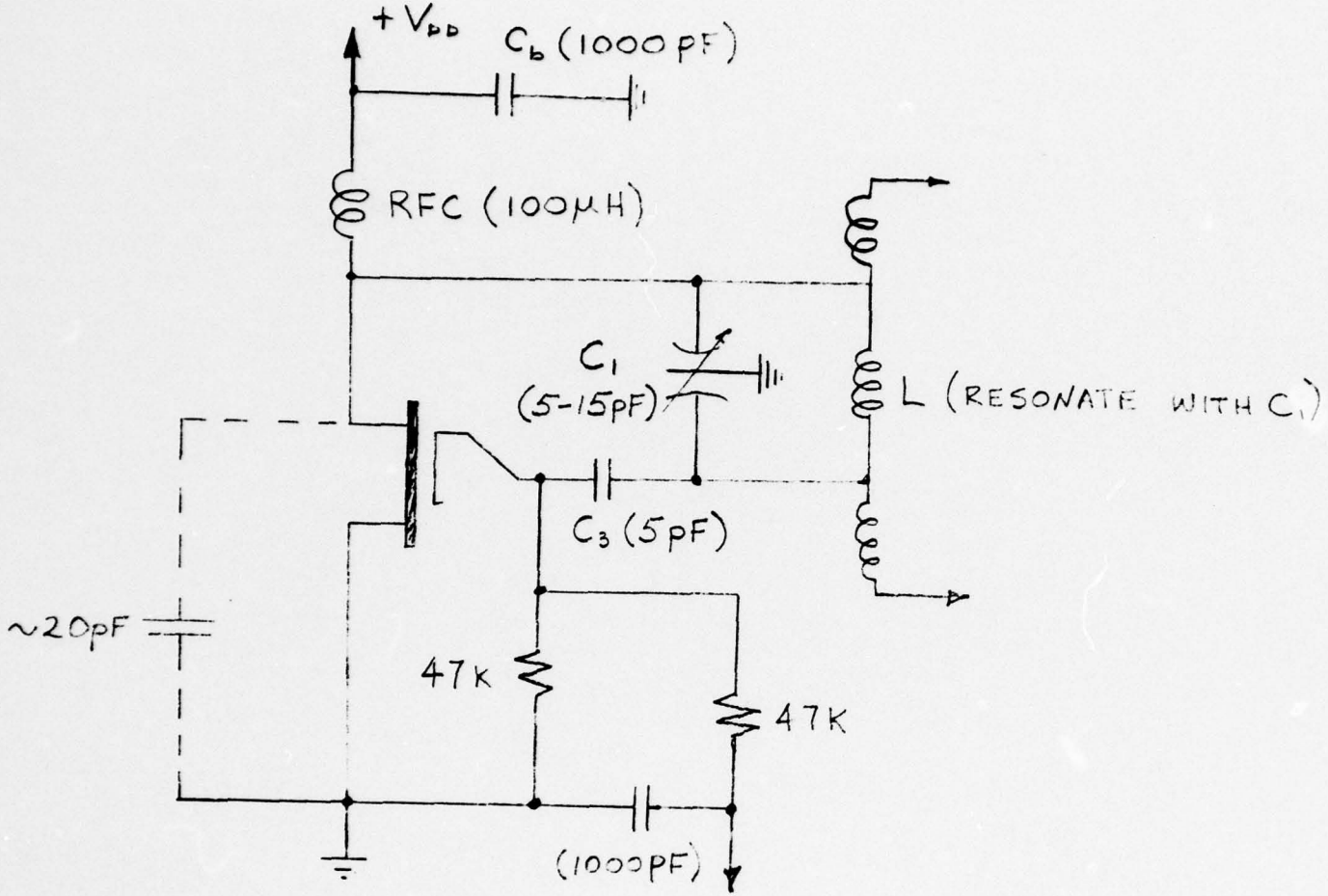

FIGURE 2. COLPITTS OSCILLATOR

incapable of spontaneous striking. In operation the discharge is exceptionally quiet and frequency stable. No more than $0.1^{o}/o$ frequency shift was observable for a ten to one load resistance change. Power output is readily controllable by varying the gate bias.

The second circuit, shown in Fig. 3, not as yet completely tested, is designed as a modified Pierce oscillator similar to the bipolar transistor oscillators commonly used in these systems. This circuit is capable of a factor of ten higher RF output voltage in high load impedance circuits and yields an output balanced with respect to ground. Since it is a grounded drain circuit the entire assembly can be constructed in a 2-inch cube exclusive of coil with the support structure as the heat sink.

B. Electrolytic Hydrogen Source

The Elhygen electrolytic hydrogen generator has now been tested for some 5000 hours at flow rates as high as $6.0(10^{-4})$ torr l/sec. Dc power supply conditions at this point are 1.8 mA at 1.25 V across the cell. The current is supplied by an op amp constant current source capable of operation in a feedback mode. The control system has generally been operated open loop. Although no degradation in performance of the generator has been observed, a strange periodic fluctuation in hydrogen throughput is apparent. The period is approximately 8 days and cannot be correlated with any apparent environmental conditions. Operation in an outlet pressure negative feedback mode will, of

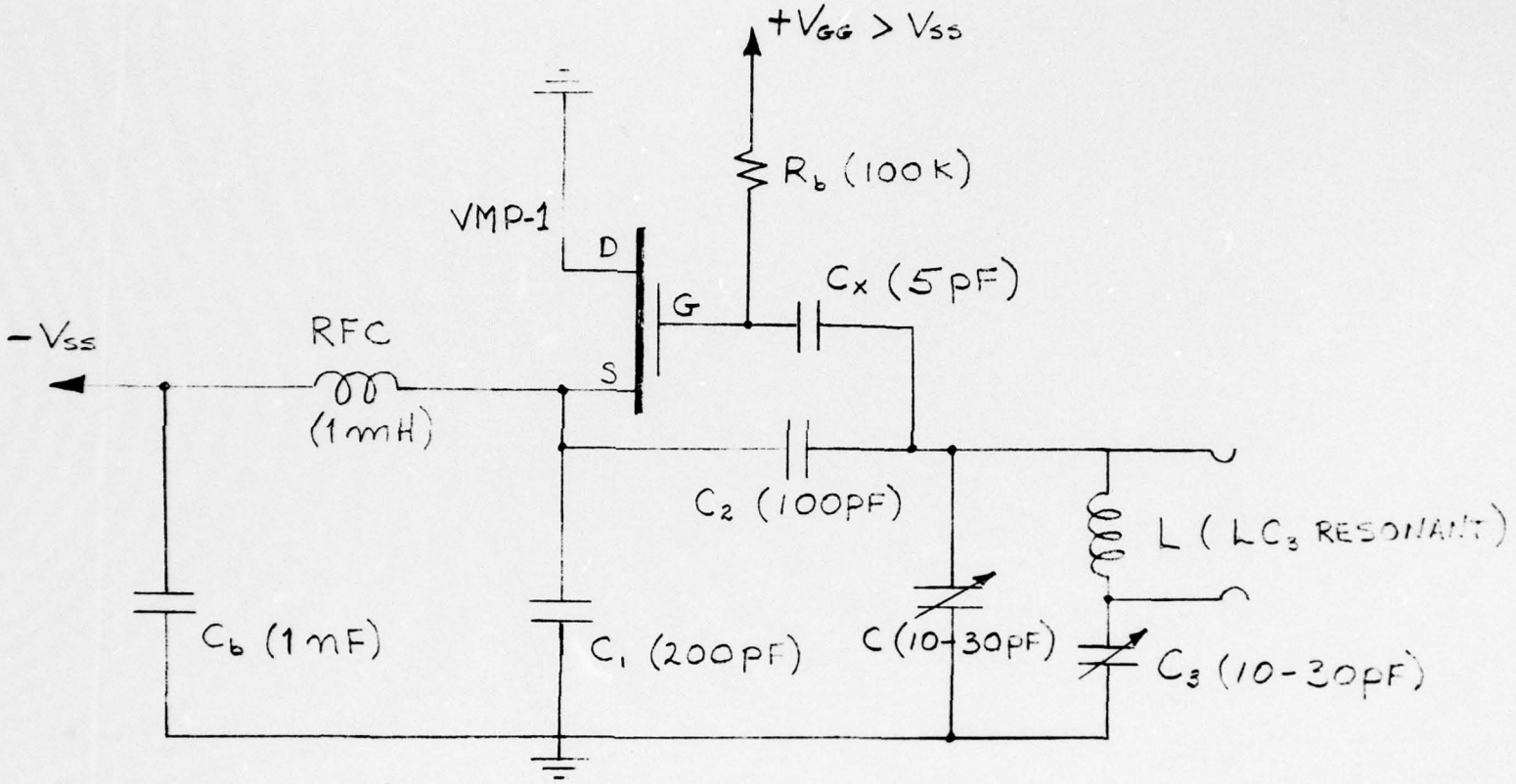

FIGURE 3 MODIFIED PIERCE OSCILLATOR

course, eliminate this condition. A slight dependence of throughput on electrolyte concentration has been observed.

Purity of the generated hydrogen appears to exceed that obtainable from previously used palladium leaks with gas reservoir and is undoubtedly superior to chemically produced hydrogen, e.g., uranium hydride.

C. Pyrex Dissociator Bulb

Testing of a 2-inch diameter pyrex dissociator bulb was initiated in late 1977. After a short time the bulb developed fractures due to stress created by uneven pressure from the stainless steel vacuum flange on which it was mounted. After considerable delay a new bulb was fabricated and put into service. The usual conditioning period during which the pressure decreased after striking the discharge was observed. After several weeks of operation at a bulb pressure of 250 mtorr the usual transition from molecular to atomic discharge was observed to occur gradually. The bulb pressure was reduced to 80 mtorr with steady state conditions remaining to this time. The atomic emission spectrum is exceptionally intense with spectral intensity ratios (atomic line ($H\beta$) to background molecular) exceeding 120. Transient measurements of bulb pressure following extinction of the active discharge indicate dissociation levels greater than $15^{o}/o$. The dissociation level is obtained by applying the theory of Section II to pressure and effusion rate changes derived from the ion pump pressure measurements.

Problems were encountered with the thin film hydrogen sensor due to inadequate shielding of the device from the electromagnetic fields of the active discharge. The situation is easily corrected and will be when testing the sapphire bulb, but this requires disassembly of the bulb flange, a procedure not warranted for the present. In any case, after the discharge is extinguished an estimate of 5×10^{14} atoms/sec was obtained from transient measurements with the sensor.

By switching off the RF discharge the ionization products rapidly recombine leaving only the neutral components, atoms and molecules. Applying the theory of Section II to this situation after steady state operation of the dissociator is attained, we find a transient relaxation of the flux from the effuser to the ion pump given by

$$F = C_e\left[0.207N_{10}(e^{-\alpha t}-e^{-qt}) + N_2{}^i\right] \text{ atoms/sec}$$

where C_e is the conductance of the effuser array, N_{10} is the atomic volume density in the dissociator bulb, $N_2{}^i$ is the unexcited steady state molecular volume density in the bulb. The time constants α and q are given by

$$q = \frac{C_e}{V_1}$$

$$\alpha = \sqrt{2}\,\frac{C_e}{V_1}\left(1 + \frac{A_i}{A_e} + \frac{2\gamma A_w}{A_e}\right)$$

where V_1 is the bulb volume ($\approx$ 100 cm^3), A_e the exit effuser effective area, A_i the inlet tube effective area, A_w the bulb wall area and γ the fraction of wall collisions resulting in

atomic recombination (first order). Inserting constants from Section II we get $q = 2.0(10^{-2})$ sec^{-1} m $\alpha = 0.17$ sec^{-1} assuming $\gamma = 2.(10^{-5})$, $N_2^{\,i} \approx 3.3(10^{15})$ mol/cm^3, and $C_e \cong 2.(10^{-3}$ cm^3/sec sec, all constants appropriate to a bulb H_2 pressure of 100 mtorr and room temperature.

Figure 4 shows the results of a measurement of F via the ion pump current which is logarithmically proportional to F. Ion pump pressure measurements yield a fractional change in pressure $\frac{\Delta P}{P_o} = \frac{.3 \pm .1}{5.3}$ and from the previous expression $\frac{\Delta P}{P_o} = \frac{.207 N_{10}^{o}}{N_2^{\,i}}$. At the initial pressure (data) of 60 mtorr this corresponds to $23 \pm 9^{o}/o$ dissociation of the original molecular component which translates to an atomic beam flux of $2.2 \pm .7(10^{15})$ atoms/sec. The atomic wall recombination coefficient seems to be approximately four times as large as reported in the literature and equal to $20.(10^{-5})$ for 7740 pyrex.

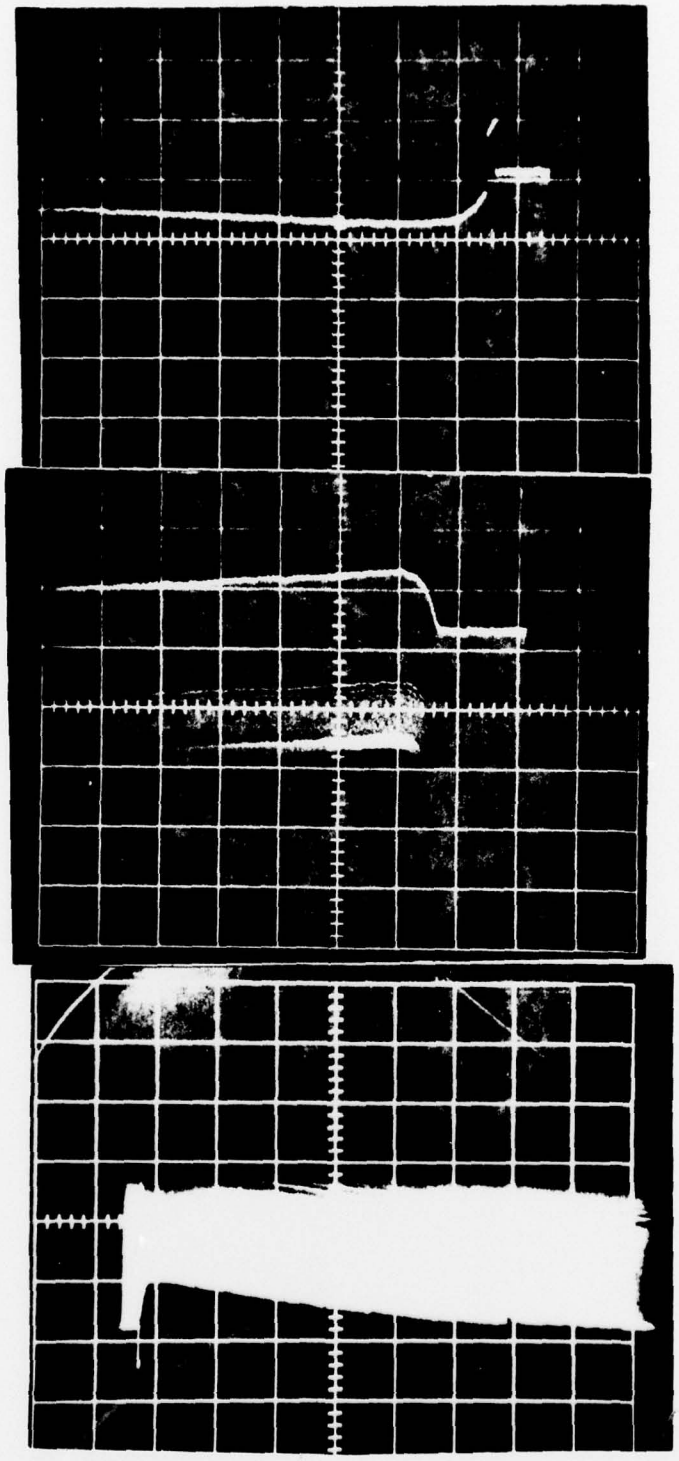

DISCHARGE OFF TRANSIENT

1 SEC/CM

t

DISCHARGE ON TRANSIENT

1 SEC/CM

t

DISCHARGE OFF (INVERTED)

5 SEC/CM

t

FIGURE 4 BULB TRANSIENT RESPONSE

REFERENCES

1. Personal communication: V. Reinhardt, Goddard Space Flight Center, Greenbelt, MD, 1977.

2. V. H. Ritz, V. M. Bermudez, V. J. Folen, Naval Research Laboratory Report, Washington, DC, 1977.

3. A. Mandl, A. Salop, J. Appl. Phys. 44, 4776 (1973).

4. M. Coulon, J. C. Fanton, L. Bonnetain, J. Chim. Phys. 70, 1493 (1973).

5. B. J. Wood, H. Wise, J. Phys. Chem 66, 1049 (1962).

6. A. B. King, H. Wise, J. Phys. Chem. 67, 1163 (1963).

7. "Fundamentals of Vacuum Science and Technology," Lewin, McGraw-Hill, 1965.

8. J. C. Greaves, J. W. Linnett, Proc. Rog. Soc. A 55, 1338 (1959).

9. T. C. Marshall, Phys. Fluids, 5, 743 (1962).

10. J. J. DeLuca, NASA Tech Brief B73-10284 (1973). U.S. Patent Office, U.S. Pat. No. 3,859,714.

11. V Hochuli, P. Holdemann, Rev. Sci. Instr. 43, 1088 (1972).